Kinetic Study of Heterogeneous Photocatalysis for Porous Nanocrystalline TiO2 Assemblies Using a Continuity Random Walk Simulation

Journal:	*Physical Chemistry Chemical Physics*
Manuscript ID:	CP-ART-05-2014-002243.R1
Article Type:	Paper
Date Submitted by the Author:	22-Jun-2014
Complete List of Authors:	liu, baoshun; Wuhan university of technology, School of material science and engineering Zhao, Xiujian; Wuhan University of Technology, Key Laboratory of Silicate Materials Science and Engineering

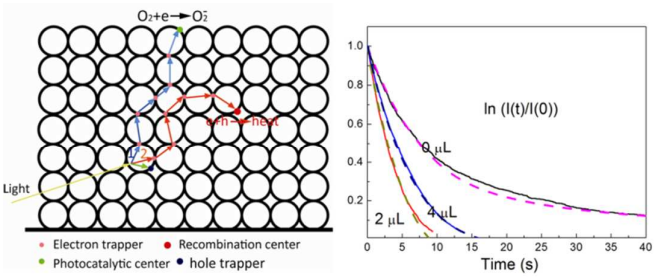

The Monte-Carlo continuous time random walk method was used to study the photocatalytic kinetic of nc-TiO_2 materials in this research.

Journal Name

RSCPublishing

ARTICLE

Kinetic Study of Heterogeneous Photocatalysis for Porous Nanocrystalline TiO_2 Assemblies Using a Continuity Random Walk Simulation

Cite this: DOI: 10.1039/xoxxoooooox

Received ooth January 2012,
Accepted ooth January 2012

DOI: 10.1039/xoxxoooooox

www.rsc.org/

Baoshun Liu,[a*] Xiujian Zhao

Continuity-*time* Random Walk (CTRW) simulation was used to study the photocatalytic kinetic of nanocrystalline (nc)-TiO_2 assemblies in this research. The nc-TiO_2 assemblies, such as nc-TiO_2 porous films and nc-TiO_2 hierarchical structures, are now widely used in photocatalysis. The nc-TiO_2 assemblies have quasi-disordered networks consisting of many tiny nanoparticles, so the charge transport within them can be studied by CRTW simulation. We considered the experimental facts that the holes can be quickly trapped and transfer to organic species just after photogeneration, and the electrons transfer to O_2 slowly and accumulate in conduction band of TiO_2, which is believed to be rate-limited process of photocatalytic kinetic under the condition of low light intensity and low organic concentration. Due to the existence of numerous traps, the electron transport within nc-TiO_2 assemblies follows multi-trapping (MT) mechanism, which significantly limits the electron diffusion speed. The electrons need to experience several steps of MT transport before transferring to oxygen, so it is highly possible that the electron transport in nc-TiO_2 networks is determined for standard photocatalytic reactions. Based on the MT transport model, the transient decays of photocurrents during photocatalytic oxidation of formic acid were studied by CRTW simulation, which are in good accordance with the experiments. The steady state photocatalysis was also simulated. The effects of organic concentration, light intensity, temperature, and nc-TiO_2 crystallinity on the photocatalytic kinetic were investigated, also in consistence with the experimental results. Due to the agreement between the simulation and the experiments for both the transient and the steady state photocatalysis, the MT charge transport should be an important mechanism that controls the kinetic of recombination and photocatalysis in nc-TiO_2 assemblies. Also, our research provides a new methodology to study the photocatalytic dynamic from the random event viewpoint, which can be revised to investigate the kinetic process of other kinds of materials.

Introduction,

Since the first publishing of Fujishima-Honda effect in 1972, [1] semiconductor heterogeneous photocatalysis has drawn much attention around the world. Its final purpose directs to deal with our concerned problems for energy shortages and environmental pollutions, [2-6] so it is still a hot research spot to date. The fabrication of highly-active photocatalysts and the utilization of visible light are two main concentrated issues. [7-9] Compared with them, the photocatalytic kinetic is complicated as it relates to many processes, including the generation, the transport, the recombination, and the interfacial charge transfer (ICT) of electrons/holes [10-12]. The theoretical full analysis needs to solve carrier continuity equations under the consideration of suitable boundary conditions. Apparently, the photocatalytic kinetic generally follows the widely-used Langmuir-Hinshelwood (L-H) model. [13-15] Although the L-H model can fit most of experimental results, it is just a "black-box" that does not disclose the kinetic behaviours of electrons and holes. Another widely-accepted microscopic mechanism is the hydroxyl free group (•OH) oxidation, [16] which was recently verified by H_2O_2 detection and fluorescence probes, [17, 18] but the origin of •OH is still in debate. The photooxidation of adsorbed H_2O molecule and OH^- ions as a •OH free radicals is accepted, but it is claimed that the photooxidation of adsorbed OH^- ions or water molecule is thermodynamically and kinetically hindered. The surface-bridged oxygen atoms of TiO_2 are considered as the primary trapping sites of the photoinduced holes and the intermediate species of H_2O photooxidation. [19, 20] Because the holes can also lead to the direct oxidization of organic species, by taking the Gerischer-Marcus ICT model

into account, the D-I (direct-indirect) model was proposed to describe photocatalytic kinetics. [21, 22] We further included the bulk recombination of electrons and holes in the D-I model and drew more reasonable results. [23] We also studied the effects of particle size, defects, geometrical structures on the photo-catalytic efficiency (PE) by using this model. [24, 25] The transient absorption spectroscopy experiments have demonstrated that the trapping of holes can occur on nc-TiO_2 within 200 fs, much faster than the electron trapping (500 ps) [26, 27]. The long lifetime of trapped holes is needed for water oxidation, which is even as long as 0.2 s in the presence of electron scavengers at neutral pH. [28, 29] The photooxidation of water as O_2 is a four-electron process, which limits the photocatalytic speed and has the non-activated feature for TiO_2 [30]. The single-hole ICT happens in the photocatalytic organic oxidation (POO), the trapped holes can quickly transfer to organic species in very short time. [31] For example, it was shown that the ICT of holes for methanol oxidation is within 300 ps [32].

The kinetic discussions on photocatalysis mainly involve the hole ICT as the holes have a direct relation with POO. The electron behaviours and their importance do not attract the same attention. As the electron ICT is slower than that of holes, the POO is generally limited by electron ICT. The time needed by the ICT of single-electron to O_2 is in the order of μs [32]. The slow electron ICT leads to obvious electron accumulation in nc-TiO_2, as shown by the in-situ photoconductivity and the absorption measurements. [33-37] nc-TiO_2 materials are the main photocatalysts used in POO. The recombination, transport, and ICT of electrons are different from that in bulk materials due to the trapping-effect. [38-39] It was shown that the electron/hole recombination in nc-TiO_2 materials is not linear, and the electron transport belongs to a thermally-activated mode. [40, 41] Many observations indicated that the electron transport in nc-TiO_2 materials should dominate the transient responses of systems. [42] Theoretically, the electron transport in nc-TiO_2 assemblies follows the multi-trapping (MT) model due to the trapping-effect. [43] Under the illumination of UV light, the photoinduced holes are quickly trapped and transfer to organic species, with the long-lived electrons being left in CB of TiO_2. The electrons are subject to multi-step MT transport within the nc-TiO_2 network before transferring to O_2. Due to the existence of MT effect, the speed of electron transport reduces two/three orders as compared to that in bulk materials. For example, the charge diffusion length is reduced to 10^{-7} cm when defects were introduced to TiO_2 surface [44]. The electron transport in nc-TiO_2 follows an activated mode, which accords to fact that most of the POO are thermally-activated. [45-47] From this point, the electron MT transport may play an important role in POO on the condition of low light intensity and low organic concentration (standard conditions), which was also verified by our theoretical research. [48] Therefore, the investigation of electron transport in nc-TiO_2 and its effect on photocatalytic kinetic is interesting.

The electron MT transport can be described as the transfer of electrons between localized traps that act as potential wells for the moving electrons. The Monte-Carlo continuous-time random-walk (CTRW) is a powerful tool for studying this in disordered or quasi-disordered media. Nelson et al. modelled electron MT transport in nc-TiO_2 electrode using a CTRW simulation and predicated that the photocurrents vary with time like t^{1-a} at long time, and that the charge recombination transients are stretched exponential in form. [49] He also got good agreement of charge recombination kinetics in dye-sensitized solar cells (DSSCs) with experiments [50]. Ansari et al. used CTRW to study the effects of morphologies and trap distributions on the electron transport in DSSCs, which predicted that 44-55 % porosities are suitable for both fast transport and dye-loading. [51] The electron MT transport in nc-TiO_2 assemblies during POO is also a stochastic process, which can be studied by CTRW, but it was seldom adopted until now. About 20 years ago, Grela et al. investigated the recombination and the reactive processes on the surface of illuminated TiO_2 colloidal particles, in which the holes perform random walks and electrons are stationary. [52] The recombination kinetic and the effects of photon flux, oxygen concentration, and particle size on the photocatalytic efficiency (PE) were simulated. Recent researches indicated that the electrons cannot be stationary in nc-TiO_2 assemblies. The free holes and shallowly-trapped holes can quickly transfer to organic species, with the deeply-trapped holes being stationary during POO. The purpose of this research is to study the intrinsic relation between the electron MT transport and the photocatalytic kinetic in nc-TiO_2 assemblies, such as nc-TiO_2 coatings and nc-TiO_2 hierarchical structures, [53, 54] from the viewpoint of random events. As the CTRW simulation gave results agreeing well with the experiments, we got a conclusion that the MT electron transport is a key electron movement mechanism in nc-TiO_2 assemblies in the course of POO, which is possible to limit the photocatalytic kinetic for standard reactive conditions.

Monte Carlo Random Walk simulation

Heterogeneous photocatalysis originates from the light excitation of semiconductors. Taken nc-TiO_2 as an example, the photogenerated holes have strong ability to oxidize many kinds of organic materials, which induces the observed photocatalytic effect. The photoinduced electrons are generally considered to be captured by oxygen and produce the super-oxygen free ions (O_2^-) and other free radicals.[55-57] The O_2^- can also induce the photocatalytic effect after some subsequent steps. [17,18] It is widely-accepted that the electron transfer to O_2 is rate-limited in photocatalysis for some n-type semiconductors with low dopants, such as nc-TiO_2. In our model, the electron transport within nc-TiO_2 materials before transferring to O_2 is important. For nc-TiO_2, the defects play a great role in the electron transport as huge amount of them exist on the surfaces or the boundaries of nc-TiO_2 materials. In the present search, we considered that the defects are exponentially distributed in the energy scale and randomly distributed spatially in TiO_2 [51].

$$g(E) = \frac{N_t}{k_B T_0} e^{\frac{E-E_C}{k_B T_0}} \quad (1)$$

where N_t, k_BT_0, and E_c are the density of traps, the characteristic energy of traps and the CB edge energy level ($E<E_c$), respectively. Before transferring to oxygen as a final aim, the electrons transport within nc-TiO_2 according to the MT model (Fig. 1 (A)). Due to the quasi-disorder of nc-TiO_2 assemblies, we treated the MT transport of electrons using a CTRW simulation, basing on which the relation between the electron MT transport and the photocatalysis was discussed.

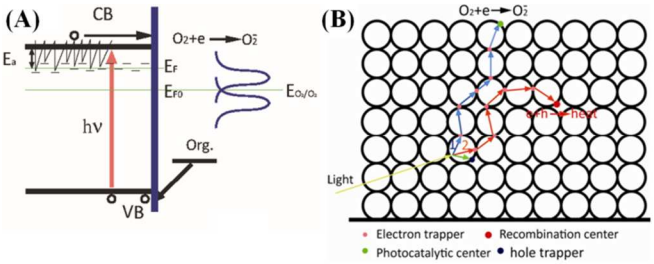

Fig. 1 (A) Diagram of electron/hole photogeneration, hole transfer to organic species, and electron MT transfer to O_2 through MT transport process; (B) Diagram of our model with using electron CTRW to simulate photocatalytic kinetic (1 denotes the electron MT transport to a photocatalytic active centre, at which the electron transfers to oxygen; 2 denotes the electron MT transport to a recombination centre, where the electron recombines with the trapped hole;3 denotes the trap of holes on nc-TiO_2 particle surface)

Fig. 1 (B) shows the photocatalytic model for Monte-Carlo CRTW Simulation. When a photon with hν higher than the E_g of TiO_2 encounters TiO_2 materials, a couple of electron and hole will be produced. Here, we assumed that the hole is quickly trapped and stationary, while the electron transports within nc-TiO_2 materials. According to the MT transport theory, the kinetics of recombination, transport, and ICT can be simulated. The numbers of electrons going to recombination and transferring to oxygen were stored during simulation, and the times needed were also stored. In the present research, computer C language was used to program the algorithm of CRTW. The number of traps was set 1.0×10^6, uniformly distributed in a 100×100×100 cubic box, with the periodic boundary condition being considered. Different from the other researches where a single-electron simulation was performed [51], the multi-electron simulation was used here in order to describe the cases more accurately. The distribution of traps with energy was constructed by using the exponentially-distributed random numbers automatically produced by computer. Fig. 2 (A) shows the trap statistic distributions with respect to energy, which are exponential functions and vary with the depth temperature T_0. A certain number of recombination centers and photocatalytic active centers were randomly set in the traps, which were labelled in the program. The electron reaching a recombination center has a probability to be recombined, and that reaching to a photocatalytic active center has a probability to transfer to oxygen. At the beginning of the simulation, the electrons were firstly randomly placed at the traps. The waiting times (detrapping times) of the electrons are given by

$$t_i = \frac{1}{\nu_0} ln(p)\, e^{-\frac{E_i}{k_B T}} \quad (2)$$

where p is a random number uniformly distributed between 0 and 1, ν_0 is the attempt to jump frequency, and its value depends on the mechanism that causes detrapping, such as electron-phonon interaction, and E_i is the energy of ith trap. Enough time of CRTW was performed to let the electrons re-distribute in the traps, finally resulting in a Fermi-Dirac distribution of thermal-equilibrium state, as shown in Fig. 2 (B). It can be seen that the Fermi level shifts to CB edge with the increase of electron number from 3000 to 50000. If an electron goes to recombination or takes part in photocatalysis, it is removed from the simulated system. For a simulation of steady photocatalysis, after an electron is consumed by recombination and photocatalysis, a new electron will be produced randomly and follows enough time Monte-Carlo CRTW relaxation. In the present research, we use n_e, n_r, n_t, p_r, p_t to denote the electron number, the recombination center number, the photocatalytic center number, the recombination probability, and the photocatalytic probability, respectively.

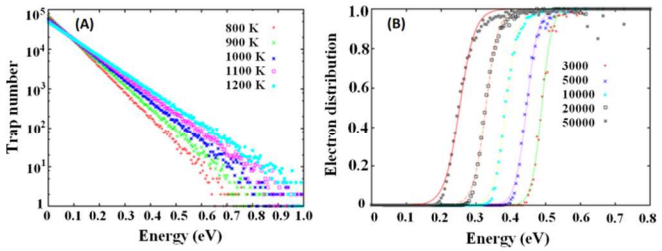

Fig. 2 Trap energies are distributed according to an exponential density of states with respect to energy for different trap depth (T_0); (B) probability that a trap of energy (E_i) are occupied in an MTRW simulation (discrete points), which fit to Fermi-Dirac distribution ($f(E_i)=1/\{1+exp[-E_i/k_BT]\}$, solid line). The calculations were carried out for systems of various numbers of particles (from 3000 to 50000) in lattices of 100×100×100.

Our simulation runs as follows:

1. A three-dimensional arrays of sites are set up.
2. Each site is given six different detrapping times (to each one of its six nearest neighbours) according to its energy according to Eqn. (2).
3. Electrons jump randomly from one site to a neighbouring site.
4. The electrons adopt the detrapping time of the sites they visits. The release (detrapping) time is then the difference between the detrapping time of the site and the time already spent by the electrons in that site
5. At each simulation step, the electron having the shortest release time is selected and allowed to jump. The release times of the rest of the carriers are then advanced by it. In the next step, the process is repeated.
6. After the Monte-Carlo CRTW reaches an equilibrium state, the simulation of photocatalysis was started. The electrons under thermal-equilibrium condition that have the shortest release time are allowed to jump. If the electron encounters a recombination or photocatalytic center, it has a probability to recombine or transfer to oxygen, and then the electron is removed from the sorted electron array.
7. A new electron is set randomly at trap sites, and new round of simulation to allow this electron to reach equilibrium. For

simulation of steady state of photocatalysis, the 6 and 7 are repeated.

Experimental

A self-made simple cell was used to measure the in-situ photocurrents during the photocatalytic oxidation of formic acid in water solution, which was shown in our previous research. [33] The setup for measuring in-situ photocurrents is shown in Fig. 3. Briefly, about 1 mm wide strip FTO film was removed from one 20 mm × 80 mm FTO glass, on which a thin film of TiO_2 nanoparticles (Commercial Degauss P25 Paste, Bought from Qicaihong Company, China) was coated by a simple blade method, which was then subjected to calcination at 450 °C for half hour. The FTO glass with a strip of TiO_2 nanoparticle film was inserted into the self-made cell, with the TiO_2 film facing up. 35 mL of deionized water that contains different amounts of formic acid (from 2 μL to 10 μL) was added in the self-made cells. Two UV fluorescent lamps (15 W, Toshiba) with an emission wavelength at 365 nm were used as the light source, which illuminated the TiO_2 film in normal direction. Variation of photocurrents with time *t* was recorded by an electrochemical workstation (CHI750, made in China) that was connected with a computer in a two-electrode mode, with a 0.5 V bias voltage being applied. Decays of photocurrents were measured by turning off lamps after the photocurrents reach steady state to study the kinetics of recombination and ICT of electrons. Based on this method, the effects of formic acid amounts and UV light intensity on steady state photocurrents was studied and compared with simulated results.

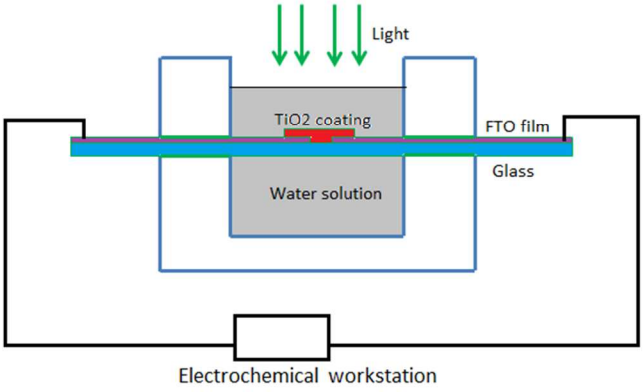

Fig. 3 Diagram for the measurement of in-situ photocurrents under the illumination of UV light

Methylene blue (MB) photo-degradation under UV light illumination was also conducted to compare with the simulation results. 2.0×10^{-5} mol L^{-1} MB water solution was used. For low concentration MB solution, it is known that the photocatalytic apparent kinetic follows a quasi-first order. The photocatalytic reaction rate constant (*k*) is used to evaluate photocatalytic activity, which is calculated according to the formula $\ln(C(0)/C(t))=kt$, with *C(0)* and *C(t)* being the initial concentration and reacted concentration at time *t*. The MB concentrations at different reaction time were decided by a UV-Vis spectrometer (UV-1601, Shimadzu, Japan), as the absorptions of MB solutions are proportional to their concentrations. Self-prepared nc-TiO_2 nanostructural materials were used. [3,58] they are poly-dispersed microspheres consisting of many nc-TiO_2 particles. 0.03 g nc-TiO_2 ethanol solutions were dispersed in ϕ 50 glass containers. After the ethanol was removed by heating at 100 °C, a thin coating of nc-TiO_2 microspheres were formed on the bottom of glass container. 50 mL MB water solution was slowly added in the glass container. UV light illuminated the nc-TiO_2 in normal direction (the UV sources were same to that used in the photocurrent measurement). The absorption spectra of MB solutions at various reaction time intervals were measured. The effects of light intensity and temperature on the photocatalytic activities were studied and compared with simulation.

Results and discussion

Transient decays of Photocurrents

Transient decays of photocurrents can reflect the kinetic mechanism of the recombination and the ICT of electrons. After the photogeneration of electrons/holes, the fast consumption of holes leads to the electron accumulation in nc-TiO_2 CB during the POO, which contributes to the photocurrents. When the light is shut off, the photocurrents will decay due to the subsequent recombination of electrons and the ICT to oxygen. As the electrons transport in nc-TiO_2 according to the MT mode, the electron mobility is not a constant, but changes with electron concentration, and the conductivity is

$$\sigma(n) = \mu(n)n \quad (3)$$

where $\mu(n)$ is the electron mobility, which is the function of Fermi level (E_F) (Taking the CB bottom as reference), *n* is the electron number.

$$\mu(n) = \mu_0 e^{-E_F/k_BT} \quad (4)$$

where μ_0 is the free electron mobility in CB. In the present research, we do not need to know the real value of μ; only the relative value was calculated. The $\mu(n)$ of nc-TiO_2 film in dark is set to unit (1). Based on the difference between the dark and the illuminated steady photocurrents, the initial $\mu(n)$ and electron number (*n*) were estimated. The CTRW was used to simulate the change of electron number, and the conductivities were calculated according to Eqns. (3) and (4). The moment when light was shut off was set to 0. The photocurrents at time 0 and t are donated as *I(0)* and *I(t)*, and the normalized photoconductivities were calculated according to $\sigma(t)/\sigma(0) = I(t)/I(0)$. The simulated and measured normalized photoconductivities were compared.

The steady photocurrents of nc-TiO_2 films in formic acid water solution are obviously higher than that in pure water, because the existence of formic acid can effectively trap holes and prohibit recombination. For 2 μL and 4 μL formic acid water solution, the steady photocurrents are ca. 10 and ca. 17 times as much as that in pure water, respectively. Fig. 4 (A) shows the decays of the photocurrents of nc-TiO_2 films. Fig. 4

(B) shows the measured (dashed line) and simulated (solid line) dependences of normalized photocurrents (*I(t)/I(0)*) on time *t*. For the photocurrent decay curve in pure water, all of electrons have to go to recombination as no photocatalytic reactions take place. The transient decay of photocurrent exhibits non-exponential dependence on time t, in agreement with other reports. [40] The complete recombination of electrons needs long time due to the trapping effect, and our CTRW simulation (solid line in Fig. 4 (B)) can well fit the experimental result. As the simulation was based on the MT electron transport, it can be known that the recombination of electrons in nc-TiO_2 film should be limited by MT transport [40], with the electron traps below CB playing a great role. [33]

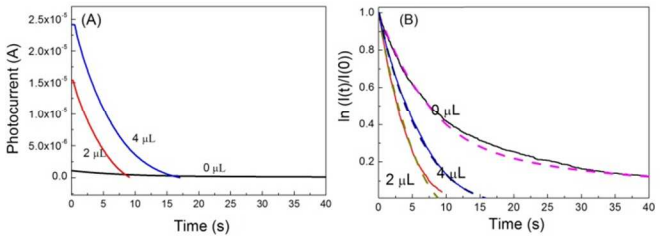

Fig. 4 (A) Photocurrent decays of nc-TiO_2 film in pure water and formic acid water solution; (B) Normalized measured (dashed lines) and simulated (solid lines) of photocurrent decay curves during photocatalytic oxidation of formic acid. The simulation carried in lattice of 100×100×100 and other different parameters. (0 μL formic acid: n_e=1000, n_r=3000, Initial n_t=0.16, n_p=1000, p_t=0, initial relative μ_n=1, N_L=1.0×10^{20} cm^3, k_BT=0.026 eV, T_0=1000 °C; 2 μL formic acid: n_e=1500, n_r=3000, Initial n_t=0, n_p=1000, p_t=0.26, initial relative μ_n= 1.3, N_L = 1.0×10^{20} cm^3, k_BT=0.026 eV, T_0=1000 °C; 4 μL formic acid: n_e=2000, n_r=3000, Initial n_t=0, n_p=1000, p_t=0.23, N_L=1.0×10^{20} cm^3, k_BT=0.026 eV, initial relative μ_n = 1.5, T_0=1000 °C;)

Steady state photocatalysis

For the steady state photocatalysis of nc-TiO_2 materials, the important factors that influence photocatalytic activities include the nc-TiO_2 features, the organic concentration, the light intensity, and the temperature. The effects of them on photocatalysis were simulated by CTRW and compared with the experimental results.

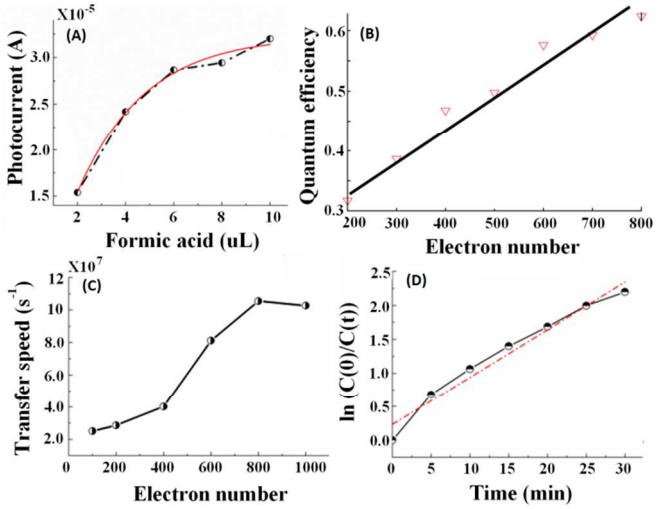

Fig. 5 (A) dependence of photocurrents on formic acid amount from 2 μL to 10 μL (in 35 ml water); (B) Simulated dependence of quantum efficiency on electron number from 200 to 800; (C) Simulated relation between electron ICT speeds and electron number from 100 to 1000. (D) Dependence of ln(*C(0)/C(t)*) on reaction time *t* during the photodegradation of MB water solution under the UV light illumination; (Simulation parameters: n_r=200, Initial n_t=0.5, n_p=200, initial p_t=0.2, N_L=1.0×10^{20} cm^3, k_BT=0.026 eV, T_0=1000 °C;)

When formic acid was added, the photocurrent decreases much faster than that in pure water, indicating that there should be the other kinetic process contributing to the photocurrent decay in addition to the recombination. Because most of holes are consumed by formic acid, there are few holes that can recombine with electrons. Because of the prohibition of recombination, the excess electrons in nc-TiO_2 CB must transfer to O_2, and its kinetic behavior is different from that of recombination. The recombination probability is just set to zero when formic acid is added. In addition, our experiment shows that the steady photocurrent also increases with the increase of formic acid amounts, so the initial electron number *(n)* and initial μ_n is set to increase as the formic acid amount increases. The absorption of formic acid on nc-TiO_2 surface may compete with that of O_2, so the probability of ICT was set to slightly decrease when the formic acid amount increases. As shown in Fig. 4 (B), the CTRW simulations are well in accordance with the experiments. These consistencies solidify our recognition that the ICT of electrons to O_2 should be determined by the MT transport in nc-TiO_2 assemblies under photocatalytic standard conditions, which support our assumption and theoretical predication in the previous studies [33, 48].

The effect of organic concentrations- Photocatalytic reactions generally follow the quasi-first-order kinetic under standard experimental conditions (low light intensity and low pollutant concentration), as shown in Eqn. (5).

$$r = \frac{dC}{dt} = k_{app}C \quad (5)$$

where k_{app} is the photocatalytic reaction rate constant, and C is the organic concentration. Under steady state, the speed of ICT of holes from VB to organic species should be proportional to pollutant concentration

$$v_h = k_h C \quad (6)$$

The photogeneration of holes is the sum of the recombination and the ICT of holes.

$$G = R + k_h C \quad (7)$$

where G is the photogeneration rate, and R denotes the recombination rate. The speed of hole ICT must be same to that of electron ICT from CB to oxygen under steady state condition. As O_2 is abundant, its concentration can be considered as constant during photocatalysis, we have

$$k_e n = k_h C \quad (8)$$

where n is the concentration of electrons in CB. Eqn. (8) means that the increase of pollutant concentration can increase the ICT of holes through increasing n and prohibiting recombination.

In our CTRW simulation, the probability for electrons to be reduced by oxygen was set to slightly decrease, as the

adsorption of organic species on nc-TiO_2 surface may affect it. The probability of hole/electron recombination was also set to decrease as the increase of pollutant concentration leads to the enhancement of recombination prohibition (Eqn. (7)). For simplicity, it was supposed that the recombination probability is inversely proportional to the pollutant concentration, as it can well accord with experiments. Based on the fact that only the electrons that locate at the traps near Fermi level can contribute to the electron transport, single-electron simulation was often used to calculate electron transport in nc-TiO_2 so as to save computing time and cost. [51] However, single-electron simulation cannot be directly used to deal with the effect of organic concentration on photocatalysis, so full-electron simulations were adopted in the present research. Moreover, the full-electron simulation can give a better simulation on the real cases than single-electron simulation, although it needs longer time (one round calculation needs ca. 24 hours for our simulations). In order to eliminate random statistical errors, at least ten times full-electron simulations were firstly performed, and the statistic average was calculated.

Fig. 5 (A) shows the dependence of steady photocurrents on the formic acid amounts. It can be seen that the photocurrent increases almost linearly for low amounts of formic acid, which tends to be saturated for high concentrations because of the saturation of formic acid adsorption on TiO_2 surface. Our result was in accordance with the results of Xie et al. and our previous study. [34, 35] As the photocurrent is proportional to the organic concentration, we simply considered that the electron number is proportional to the organic concentration under steady state conditions, according to Eqn. (8). Due to this fact, we simulated the variation of quantum efficiency (QE) with the electron number. Here, QE was calculated as the division between the number of ICT electrons and the whole generated electrons. Fig. 5 (B) shows the dependence of simulated QE on the electron number, which increase linearly when the electron number increases. Since the electron number is proportional to the organic concentration, so the steady CTRW simulation demonstrates a linear relation between the photocatalytic activity and the organic concentration, which accords with the quasi-first-order kinetic (Eq. (5)) and is supported by many experiments. In addition, the relation between the speeds of electron ICT (photocatalytic speed) and the electron number (n) was also simulated, as shown in Fig. 5 (C). It also shows a quasi-linear relation between the ICT speeds and the electron number (The ICT speed was calculated by dividing the ICT electron number with the time used). The photocatalytic degradations of MB water solutions under the UV light illumination were performed, as shown in Fig. 5(D). As the dependence of ln($C(0)/C(t)$) on time t has a linear mode, the experiment results are in agreement with our simulation results.

The effect of Light intensity-The photocatalytic activity generally increases with the increase of light intensity. However, the effect of light intensity on photocatalysis is different from that of organic concentration, as the variation of light intensity can both change the holes and the electrons. According to our assumption, since the holes are trapped or transfer to organic species, the effect of light intensity on the electron concentration can be determined. Fig. 6 (A) shows the relation between the photocurrents of nc-TiO_2 porous films and the light intensity, with the formic acid amount being unchanged (4 μL in 35 mL water). The photocurrents increase linearly with the increase of light intensity and tend to reach be saturated for high light intensity, also in accordance with other reports. [34] The result shows that it can be simply considered that n is proportional to light intensity for standard experimental conditions (Low light intensity). Because the hole concentration increases when the light intensity increases, the recombination probability was set to increase as the electron number increases. Fig. 6 (B) shows the variation of QE with electron number, which decreases when light intensity increases. Our CTRW simulation result is in good consistence with other experimental results [15] and theoretical predication. [21, 22] This simulation clearly supports our general recognition that the increase of light intensity can reduce the QE by increasing recombination probability, from a random event microscopic viewpoint.

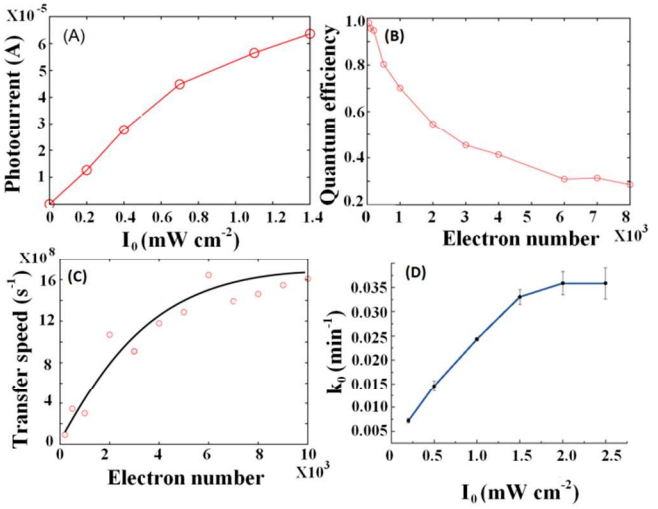

Fig. 6 (A) dependence of photocurrents on the light intensity with the addition of 4 μL formic acid; (B) Simulated dependence of quantum efficiency on the electron number; (C) Simulated relation between the electron ICT speeds and the electron number. (D) Dependence of photocatalytic reaction rate constant (k_0) on the light intensity (I_0) during the photo-degradation of MB water solutions under UV light illumination; (Simulation parameters : n_r=200, initial n_t=0.2, n_p=200, initial p_t=0.2, N_L=1.0×10^{20} cm^3, k_BT=0.026 eV, T_0=1000 °C;)

In addition, we also simulated the dependence of electron ICT speed on the light intensity, as shown in Fig. 6 (C). It can be seen that the ICT speed firstly increases with the increase of light intensity, and then reaches a saturated level, which is different from Fig. 5 (C). According to our physical model, the traps have exponential distribution with respect to energy, and the electron MT transport within nc-TiO_2 network limits the ICT of electrons. According to Fig. 2 (B), the effect of electron number on the change of Fermi level becomes smaller and smaller with the increase of electron number, resulting in the dependence of ICT speed on n of Fig. 6 (C). This simulated result also accords with other published results. For example, basing on the •OH oxidation mechanism, Ollis et al. deduced a

square-foot relation between photocatalytic speed and light intensity. [16] Salvador et al. took the ICT of hole into consideration, and proposed that the variation of photocatalytic speed with light intensity is the mixed result of direct ICT and indirect ICT hole, which leads to a result that the relation between photocatalytic speed and light intensity has the same tendency as Fig. 6 (C). [21,22] In additional, Emeline et al. studied the relation between light intensity and the photocatalytic speed experimentally. The effect of light intensity on the photocatalytic activity of phenol decomposition was measured, which also supports our simulation. [15] Here, the photo degradations of MB water solutions under different intensity of UV light illumination were performed. The apparent rate constants (k_0) were calculated according to the L-H kinetic model. Fig. 6 (D) shows the dependence of k_0 on the light intensity. It can be seen that the relation between the light intensity (I_0) and the k_0 is in accordance with Fig. 6 (C).

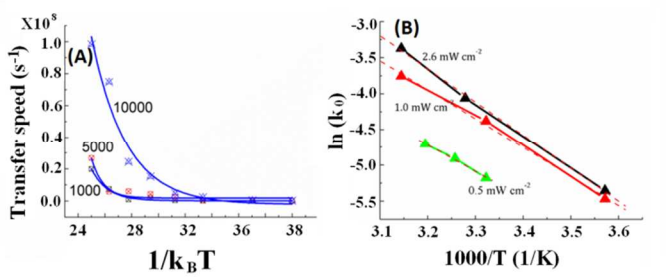

Fig. 7 (A) Simulated dependences of electron ICT speeds on $1/k_BT$ for different electron number; (B) Experimental dependences of $\ln(k_0)$ on $1000/T$ for different light intensity (Simulation parameters : n_r=200, p_t=0.2, n_p=200, p_t=0.2, N_L=1.0×10^{20} cm^3, T_0=1000 °C;)

The effect of Temperature-It is seen that the photocatalytic activities generally increase with the increase of temperature. According to our CTRW model, we also simulated the effect of temperature on the speed of electron ICT. Fig. 7 (A) shows the dependences of ICT speeds of electrons on $1/k_BT$ in the case of different electron number. As the photocatalysis is generally limited by electron ICT, it can be known that the variation of photocatalytic activity with temperature follows exponential model, indicating that the photocatalysis belongs to a thermally-activated process, which is in accordance with published results. [47,59, 60] The photo-degradations of MB water solutions at different temperatures were performed. The photocatalytic rate constant k_0 was used to evaluate photocatalytic activity. The relations between $\ln(k_0)$ and $1000/T$ plotted in Fig. 7 (B) are linear. It can be known that the MB photocatalysis is thermally-activated, also according with our simulation result. In principle, it is considered that the photocatalysis should be a non-activated process as heat cannot produce electrons/holes enough to induce the photocatalytic effect. Our model is based on the MT electron transport, which belongs to the thermally-activated process. Since it is possible for the electron-O_2 ICT to limit the photocatalytic oxidations, the activation mechanism of POO may be controlled by the MT transport of electron under the condition of low light intensity and low organic concentration. Shimura et al. used β-Ga_2O_3 to produce hydrogen from water by using sacrificial agent to trap holes, and found that the kinetic and the activation mechanism of hydrogen production follows electron MT transport, [61] which strongly supports our simulation result.

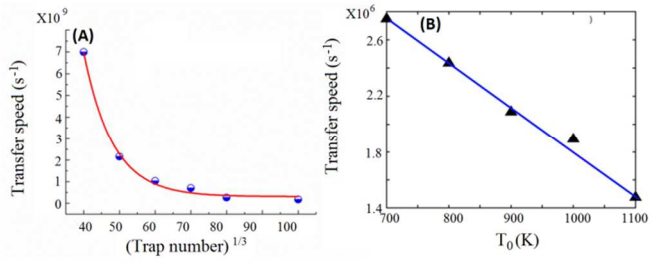

Fig. 8 (A) Simulated dependence of electron ICT transfer speeds on the trap number; (B) Simulated dependence of electron ICT speeds on the trap depth parameter (T_0) (Simulation parameters : n_e=2000, n_r=200, n_t=0.2, n_p=200, p_t=0.2, N_L=1.0×10^{20} cm^3, k_BT=0.026 eV, T_0=1000 °C)

The effect of photocatalysts-The effect of nc-TiO_2 crystallinity on photocatalytic activity can be studied by our model. Trap number (N_L) and trap depth (T_0) are two main parameters that can be tuned to simulate the change of TiO_2 crystallinity. The N_L will decrease, and the T_0 will increase when the nc-TiO_2 crystallinity increases, which can be tuned by experiments. Fig. 8 (A) shows the dependence of electron ICT speeds on the trap number. The simulation result clearly shows that the ICT speed increases with the decrease of trap number. When the trap number increases, more electrons will be trapped and become immobilized. The number of electrons transferring to O_2 decreases, leading to the decrease of photocatalytic activity. Fig. 8 (B) shows the relation between the electron ICT speeds with the trap depth, it can also be seen that the ICT speeds decrease as T_0 increases. As the increase of T_0 enhances the depth of trap distribution (Fig.2 (A)), more electrons will be trapped in deep traps for higher T_0. These electrons need long time to be deactivated and cannot contribute to photocatalysis, so the photocatalytic activities decrease. The simulation results are also well in accordance with many experimental results. For example, Joo et al. used a novel partial etching and re-calcination process to prepare mesoporous hollow TiO_2 shells with controllable crystallinity. [62] The photo-degradation of rhodamine B under UV light irradiation was used to evaluate the photocatalytic activity, showing that the photocatalytic activity increases as the crystallinity increases. Othman et al. systematically studied the effects of crystallinity and size of nc-TiO_2 on the photocatalytic activity (photodegredation of MB). It was shown that the photocatalytic activity increases with the increase of crystallinity. [63] Many other researches also reports that the increase of nc-TiO_2 crystallinity can increase the photocatalytic activity. [64, 65] Recently, we prepared nano-TiO_2 mesoporous films on soda-glass surface, and showed that the photocurrents and the POO of acetone increase with the increase of crystallinity. [66] Generally, it is considered that the

increase of crystallinity can reduce the recombination centers, so resulting in the improvement of photocatalytic activity. In additional to the decrease of recombination centers, our simulation clearly shows that the crystallinity increase can accelerate the electron transport to O_2 through reducing the trap number and the trap depth, leading to the effective prohibition of recombination and the increase of photocatalytic activity.

Conclusions

Based on the MT electron transport, the photocatalytic kinetic of nc-TiO_2 assemblies was studied by a CTRW simulation. The kinetics of recombination and ICT of electrons were studied through the measurement of photocurrent decays of nc-TiO_2 coating during the POO of formic acid. The CTRW simulations can well accord with the photocurrent decays, indicating that the MT transport of electrons in nc-TiO_2 plays an important role in the recombination and the ICT during the POO under the standard conditions. The effects of organic concentration, light intensity, temperature, and nc-TiO_2 crystallinity on the photocatalytic kinetic were also studied by the CTRW simulation, which are in agreement with the experiments. The consistencies between the simulation and the experiments indicate that there should be an intrinsic relation between the POO and the electron transport in nc-TiO_2 assemblies. We considered that the electrons must experience several steps of MT transport before transferring to O_2, which can be rate-limited for photocatalytic kinetic under the standard conditions (low concentration and low light intensity). Our simulation also indicates that the enhancement of electron transport in nc-TiO_2 assemblies may be effective to increase photocatalytic activity. The present research also provides an alternative way to study photocatalytic kinetic, from the viewpoint of random event, which can be extended to the other kinds of materials.

Acknowledgements

B. Liu thanks the National Basic Research Program of China (2009CB939704), and Fundamental Research Funds for the Central Universities (Wuhan University of Technology, 2013-II-017).

Notes and references

[a] State Key Laboratory of Silicate Materials for Architectures, Wuhan University of Technology, Hubei Province, Wuhan, 430070, China
Corresponding author: Dr. B. Liu, liubaoshun@126.ocm

1 A. Fujishima, K. Honda, *Nature*, 1972, **238**, 37–38.
2 K. Nakata, A. Fujishima, *J. Photochem. Photobiol., C*, 2012**, 13**, 169-189.
3 B. Liu, K. Nakata, M. Sakai, H. Saito, T. Ochiai, T. Murakami, K. Takagi, A. Fujishima, *Catal. Sci. Technol.*, 2012, **2**, 1933-1939.
4 K. Hashimoto, H. Irie, A. Fujishima, *Jpn. J. Appl. Phys.,* 2005, **44**, 8269-8285.
5 M. R. Hoffmann, S. T. Martin, W. Choi, D. W. Bahnemann, *Chem. Rev.*, 1995, **95**, 69-96.
6 Y. Qua, X. Duan, *Chem. Soc. Rev.*, 2013, **42**, 2568-2580.
7 V. Etacheri, M. K. Seery, S. J. Hinder, S. C. Pillai, *Chem. Mater*., 2010, **22**, 3843-3853.
8 W. Zhou, H. Liu, J. Wang, D. Liu, G. Du, J. Cui, *ACS Appl. Mater. Interfaces*, 2010, **2**, 2385-2392.
9 N. Wu, J. Wang, D. N. Tafen, H. Wang, J. G. Zheng, J. P. Lewis, X. Liu, S. S. Leonard, A. Manivannan, *J. Am. Chem. Soc*., 2010, **132**, 6679-6685.
10 J. Wang, D. N. Tafen, J. P. Lewis, Z. Hong, A. Manivannan, M. Zhi, M. Li, N. Wu, *J. Am. Chem. Soc*., 2009, **131**, 12290-12297.
11 K. Nakata, T. Ochiai, T. Murakami, A. Fujishima, *Electrochim. Acta,* 2012, **84**, 103-111.
12 S. O. Obare, T. Ito, G. J. Meyer, *J. Am. Chem. Soc*., 2006, **128**, 712-713.
13 B. Liu, X. Zhao, C. Terashima, A. Fujishima, K. Nakata, *Phys. Chem. Chem. Phys.*, 2014,**16**, 8751-8760.
14 D. F. Ollis, *J. Phys. Chem. B*, 2005, **109**, 2439-2444.
15 A. Emeline, V. K. Ryabchuk, N. Serpone, *J. Phys. Chem. B*, 2005, **109**, 18515-18521.
16 C. S. Turchi, D. F. Ollis, *J. Catal.*, 1990, **122**, 178-192.
17 J. Zhang, Y. Nosaka, *J. Phys. Chem. C.* , DOI: 10.1021/jp501214m
18 V. Diese, M. onsson, *J. Phys. Chem. C.* , DOI: 10.1021/jp500315u
19 P. Salvador, *Prog. Surf. Sci.,* 2011, **86**, 41-58
20 J. F. Montoya, I. Ivanova, R. Dillert, D. W. Bahnemann, P. Salvador, J. Peral, *J. J. Phys. Chem. Lett.* 2013, **4**, 1415-1422.
21 T. L. Villarreal, R. Gómez, M. González, P. Salvador, *J. Phys. Chem. B,* 2004, **108**, 20278-20290.
22 I. Mora-Seró, T. L. Villarreal, J. Bisquert, Á. Pitarch, R. Gómez P. Salvador, *J. Phys. Chem. B,* 2005, **109**, 3371-3380.
23 B. Liu, X. Zhao, *Electrochim. Acta*, 2010, ***55***, 4062-4070.
24 B. Liu, K. Nakata, S. Liu, M. Sakai, T. Ochiai, T. Murakami, K. Takagi, A. Fujishima, *J. Phys. Chem. C*, 2012, **116**, 7471-7479.
25 B. Liu, K. Nakata, X. Zhao, T. Ochiai, T. Murakami, A. Fujishima, J. *Phys. Chem. C*, 2011, **115**, 16037-16042.
26 X. Yang, N. Tamai, *Phys. Chem. Chem. Phys.*, 2001, **3**, 3393–3398.
27 Y. Tamaki, A. Furube, M. Murai, K. Hara, R. Katoh, M. Tachiya, *Phys. Chem. Chem. Phys.,* 2007, **9**, 1453-1460.
28 J. W. Tang, J. R. Durrant, D. R. Klug, *J. Am. Chem. Soc.*, 2008, **130**, 13885-13891.
29 A. J. Cowan, J. W. Tang; W. H. Leng, J. R. Durrant, D. R. Klug, *J. Phys. Chem. C,* 2010, **114**, 4208–4214.
30 A. J. Cowan, C. J. Barnett, S. R. Pendlebury, M. Barroso, K. Sivula, M. Grätzel, J. R. Durrant, D. R. Klug, *J. Am. Chem. Soc.*, 2011, **133**, 10134-10140
31 H. H. Mohamed, D. W. Bahnemann, *Appl. Catal. B: Environ.* 2012, **128,** 91-104,
32 Y. Tamaki, A. Furube, M. Murai, K. Hara, R. Katoh, M. Tachiya, *J. Am. Chem. Soc*., 2006, **28**, 1416-1417.
33 A. Yamakata, T. Ishibashi, H. Onishi, *J. Phys. Chem. B*, 2001, **105**, 7258-7262.
34 B. Liu, X. Wang, L. Wen, X. Zhao, *Chem. – A Euro. J.*, 2013, **19**, 10751-10759.
35 S. Zhang, C. Xie, Z. Zou, L. Yang, H. Li, S. Zhang, *J. Phys. Chem. C*, 2012, **116**, 19673-19681.
36 L. Zhang, H. H. Mohamed, R. Dillert, D. Bahnemann, *J. Photochem. Photobiol. C,* 2012,**13,** 263-276.

37 H. H. Mohamed, C. B. Mendive, R. Dillert, D. W. Bahnemann, *J. Phys. Chem. A*, 2011, **115**, 2139-2147.
38 J. Bisquert, *J. Phys. Chem. C,* 2007, **111**, 17163-17168.
39 M. Grünewald, B. Movaghar, B. Pohlmann, D. Würtz, *Phys. Rev. B.,* 1995, **32**, 8191-8196.
40 J. A. Anta, *Energy Enviorn. Sci.*, 2009, **2**, 387-392.
41 J. A. Anta, I. Mora-seró, T. Dittrich, J. Bisquert, *J. Phys. Chem. C,* 2007, **111**, 13997-14000.
42 M. Ansri-Rad, J. A. Anta, J. Bisquert, *J. Phys. Chem. C,* 2013, **117**, 16275-16289.
43 T. Berger, D. Monllor-Satoca, M. Jankulovska, T. Lana-Villarreal, R. Gómez, *ChemPhysChem,* 2012, **13**, 2824-2875.
44 P. Salvador, J. *Appl. Phys.*, 1984, **55**, 2977-2985.
45 K. Hofstadler, R. Bauer, S. Novalic, G. Heisler, *Environ. Sci. Technol.,* 1994, **28,** 670-674.
46 A. Mills, S. Morris, *J. Photochem. Photobiol. A Chem*., 1993, **71**, 75-83.
47 G. Alsayyed, J. C. D'Oliveira, P. Pichat, *J. Photochem. Photobiol. A: Chem.*, 1991, **58**, 99-114.
48 B. Liu, *J. Electrochem. Soc.*, 2013, **160***,* H591-H596.
49 J. Nelson, R. E. Chandler, *Coord. Chem. Rev.*, 2004, **248**, 1181-1194.
50 J. Nelson, *Curr. Opin. Solid State Phys*. 2002, **6**, 87-95.
51 M. Ansari-rad, Y. Abdi, E. Arzi, *J. Phys. Chem. C*, 2012,**116,** 3212-3218.
52 M. A. Grela, A. J. Colussi, *J. Phys. Chem.,* 1996, **100**, 18214-18221.
53 S.-C. Yang, D.-J. Yang, J. Kim, J.-M. Hong, H.-G. Kim, I.-D. Kim, H. Lee, *Adv. Mater.,* 2008, **20**, 1059-1064
54 P. S. Archana, R. Jose, C. Vijila, S. Ramakrishna, *J. Phys. Chem. C,* 2009, **113,** 21538-21542.
55 X. Qiu, M. Miyauchi, H. Yu, H. Irie, K. Hashimoto, *J. Am. Chem. Soc.,* 2010, **132**, 15259-15267.
56 H. Yu, H. Irie, Y. Shimodaira, Y. Hosogi, Y. Kuroda, M. Miyauchi, K. Hashimoto, *J. Phys. Chem. C,* 2010, **114**, 16481-16487.
57 M. Liu, X. Qiu, M. Miyauchi, K. Hashimoto, *Chem. Mater.,* 2011, **23**, 5282-5286.
58 B. Liu, X. Zhao, K. Nakata, A. Fujishima, *J. Mater. Chem. A*., 2013, **1**, 4993-5000.
59 K. Hofstadler, R. Bauer, S. Novalic, G. Heisler, *Environ. Sci. Technol.*, 1994, **28**, 670-674.
60 A. Mills, S. Morris, *J. Photochem. Photobiol. A Chem.,* 1993, **71**, 75-83.
61 K. Shimura, K. Maeda, H. Yoshida, *J. Phys. Chem. C*, 2011, **115,** 9041-9047
62 J. B. Joo, Q. Zhang, M. Dahl, I. Lee, J. Goebl, F. Zaera, Y. Yin. *Energy Environ. Sci.*, 2012, **5**, 6321-6327.
63 S. H. Othman, S. A. Rashid, T. I. M. Ghazi, A. Norhafizah, *J. Nanomater.*, 2010**,** Article ID 512785.
64 S. Watson, D. Beydoun, J. Scott, R. Amal, *J. Nanoparticle Res.,* 2004, **6**, 193-207.
65 K. Tanaka, M. F. V. Capuleb, T. Hisanaga, *Chem. Phys. Lett.*, 1991, **187**, 73-76.
66 Briefly, we used sol-gel and dip-coating methods to prepare porous nc-TiO2 films on glass substrates, which was subjected to calcination at various temperature, with polyvinylpyrrolidone (PVP) being used as modification. The POO of acetone was used to evaluate the photocatalytic activity. We found that the photocurrents and the photocatalytic activity increases with the increase of calcination temperature.